



## Crystallographic, chemical and structural characteristics of harmotome from Zlatolist, Eastern Rhodopes, Bulgaria

R. Atanassova<sup>1\*</sup>, R. D. Vassileva<sup>1</sup>, M. Kadiyski<sup>2</sup>, Z. Zlatev<sup>3</sup>

<sup>1</sup> Geological Institute, Bulgarian Academy of Sciences, 1113 Sofia;

<sup>2</sup> Institute of Mineralogy and Crystallography, Bulgarian Academy of Sciences, 1113 Sofia;

<sup>3</sup> Bulgarian Mineralogical Society, Sofia

Received February 15, 2012; Revised March 15, 2012

Large volumes of intermediate and acid volcanoclastic rocks were formed during the Paleogene in the Eastern Rhodopes, South Bulgaria. Most of them were deposited in a shallow marine environment, lately transformed into clays, adularia, opal-CT and zeolites. Rare mineralization was observed in voids and cavities of basaltic rocks near the Zlatolist village. The voids, now amygdales are filled by calcite, quartz and several zeolites (harmotome, analcime, mordenite, heulandite etc.). Among these harmotome occurs as remarkably well-defined crystals up to 3.5 cm in size.

Harmotome has been characterized using optical microscopy, X-ray, SEM/EDS, EPMA, LA-ICP-MS and DTA. The investigated crystals invariably consist of complex penetration twins and twinning simulates pseudo-orthorhombic forms according to the morvenite law. Crystals are elongated along the a-axis, and flattened on the {010}. Such complex twinning results in an optical heterogeneity and characteristic uneven extinction.

The average chemical formula is:  $\text{Ba}_{2.46}\text{Ca}_{0.17}\text{K}_{0.26}[\text{Al}_{5.89}\text{Si}_{10.19}\text{O}_{32}]\cdot 12\text{H}_2\text{O}$ . Registered are 35 trace elements, up to 1.3 wt.% Na, 330 ppm Sr, and 26 ppm Ti. The thermal behavior of harmotome represents water loss in three steps: at 125, 210, and 280 °C, and complete dehydration at 400 °C.

A crystal fragment of harmotome was used also for single crystal X-ray diffraction study. Reliable structure model with satisfactory R-values ( $R_1 = 0.0403$ ;  $R_{\text{all}} = 0.0473$ ) was obtained using the P2/m space group and it was chosen for the structure refinement. The obtained unit cell dimensions are:  $a = 9.8903(5)$ ,  $b = 14.1394(3)$ ,  $c = 8.6713(4)$  Å,  $\beta = 124.628(7)^\circ$  and  $V = 997.81(8)$  Å<sup>3</sup>. The final refinement included all atomic coordinates and anisotropic thermal displacement parameters.

**Key words:** zeolites, phillipsite series, harmotome, crystal structure refinement, crystal morphology.

### INTRODUCTION

Zeolites are crystalline hydrated aluminosilicates of the alkali and alkaline elements. They have a framework structure characterized by the presence of interconnected channels or cages, occupied by relatively large cations and water molecules [1]. Depending on their structure and composition, zeolites are widely used as sorbents, detergents, ion-exchangers, and especially as materials for heterogeneous catalysis [2]. Large zeolite crystals provide an ideal possibility for crystal structure determinations [3], studies of the crystal growth mechanism [4], adsorption and diffusion measurements, and more recently spatially resolved probing of catalytic events [5].

Harmotome  $\text{Ba}_2(\text{Ca}_{0.5}\text{Na})_4[\text{Al}_5\text{Si}_{11}\text{O}_{32}]\cdot 12\text{H}_2\text{O}$  and phillipsite  $\text{K}_2(\text{Ca}_{0.5}\text{Na})_4[\text{Al}_6\text{Si}_{10}\text{O}_{32}]\cdot 12\text{H}_2\text{O}$  are members of a continuous series with exchangeable cations from barium to potassium. Considerable calcium and sodium content is commonly present. Barium is the most abundant extra-framework cation in harmotome. The name harmotome (after Häüy, 1801, in Combs *et al.* [6]) predates phillipsite; on grounds of history and usage, both are retained in spite of the rules of the report of the CNMMN [6]. Named from Greek words for a “joint” and “to cut”, in allusion to a tendency to split along junctions (twin planes). It is well known that crystal individuals invariably consist of complex twins, and Deer *et al.* [7] suggest that the twinning may simulate single crystal forms (mimetic twins), such as tetragonal and rhombic dodecahedra. Sahama and Lehtinen [8] described sectorial twinning in harmotome from Finland. Akizuki [9, 10] has interpreted sector twinning in some minerals in terms of atomic order-

\* To whom all correspondence should be sent:  
E-mail: radi@geology.bas.bg

ing of such cations as Al/Si and  $\text{Fe}^{3+}/\text{Al}$ , produced during growth. The surface and internal textures of harmotome suggest that the sectorial twinning may originate by the same mechanism. Untwinned crystals have not been found so far. A transparent, spindle-shaped variety of harmotome that was originally described from the Strontian mines north of Morven (now Morvern), Argyllshire, Scotland, UK [11], later was used to describe a type of twinning also observed for phillipsite. The complex interpenetration twinning of phillipsite was classified by Lacroix (1897, 1923 in: Tschernich [12]) to include the Morvenite twin, Marburg twin, Perier twin and Stempel twin according to the dominant habits.

Harmotome is typically monoclinic, although its actual space group is debatable due to acentricity, which is lowering the symmetry [13]. Harmotome and phillipsite have the same (structural code, PHI) framework topology with double “crankschafts” parallel to the  $a$ -axis.

Until now harmotome was known from one occurrence in Bulgaria. It was described from fissures of latitic lavas North of Iskra, Haskovo district with laumontite and heulandite [14]. In this study, we present the crystallographic, mineralogical and chemical data on harmotome from Zlatolist, Eastern Rhodopes. In addition, the val-

ues of the cell parameters are obtained by single-crystal X-ray diffractometry.

## GEOLOGICAL OVERVIEW

Intense collision-related volcanism took place in the East Rhodopes, South Bulgaria during the Paleogene. Eruptive products, both lava and volcanoclastic rocks, are assigned to four intermediate (to basic) phases alternating in time with five acidic ones [15]. The first two phases (intermediate and acidic) are Priabonian while all following are of Rupelian age. Large volumes of pyroclastic rocks were erupted during the first three acidic volcanic phases and deposited in a shallow marine environment. They were subsequently transformed into zeolites, clay minerals, adularia and opal-CT [15].

Rare zeolite mineralization was observed in voids and in some microdruses and cavities of basaltic andesites near the Zlatolist village, Eastern Rhodopes (Fig. 1). The voids, now amygdales are filled predominantly by calcite, quartz, chalcedony and several zeolites (mainly represented by harmotome, analcime, chabasite, mordenite and heulandite). Among these zeolites, harmotome occurs as remarkably well-defined large crystals.



**Fig. 1.** Photographs of: a) outcrop of basaltic rocks near Zlatolist, b-d) handspecimens representing large harmotome crystals in amygdales

## EXPERIMENTAL AND ANALYTICAL PROCEDURES

Harmotome has been characterized using optical microscopy, X-ray diffraction, SEM/EDS, EPMA, LA-ICP-MS and DTA.

Detailed morphological studies on separate crystals and aggregates were carried with a binocular optical and scanning electron microscopes JEOL JSM 6390 with EDS Oxford INCA system (SEM). Electron probe microanalyses (EPMA) were performed with a JEOL JSM CF with Tracor Northern – 2000 analyzing system at an accelerating voltage of 25 kV and a beam diameter of 1  $\mu\text{m}$ . Electron microprobe analyses are performed on the same samples used for the structure determination. In each crystal, several spots were analyzed to check for sample homogeneity.

LA-ICP-MS analytical system consists of a 193 nm ArF excimer laser and an ELAN DRC-e ICP quadrupole mass spectrometer. For controlled ablation, an energy density of above 10 J/cm<sup>2</sup> on the sample and a laser pulse frequency of 10 Hz were used. Analyses were performed with 50 or 75  $\mu\text{m}$  beam diameters and external standardization on NIST glass standard SRM-610.

TG-DTA-DTG measurements were performed in air with heating rate 10 °C/min.

The powder diffraction patterns of harmotome were measured on a D2 Phaser Bruker AXS at room temperature with Ni-filtered Cu-K $\alpha$  radiation ( $\lambda = 1.5406 \text{ \AA}$ ). Data was collected in step-scan mode from 4 to 70  $^{\circ}2\theta$  with 0.05  $^{\circ}2\theta$  step and 1s exposure time.

## CRYSTAL STRUCTURE

A single crystal of harmotome from Zlatolist with dimensions 0.25  $\times$  0.22  $\times$  0.20 mm was mounted on a glass fibre and measured on an Oxford diffraction Supernova diffractometer equipped with Atlas CCD detector. X-ray data collection was carried out at room temperature with monochromatic Mo-K $\alpha$  radiation ( $\lambda = 0.71073 \text{ \AA}$ ). After the initial matrix procedure, a C-centred unit cell (Laue class *mmm*) with parameters  $a = 9.9034(5)$ ,  $b = 14.2979(9)$ ,  $c = 14.1612(7) \text{ \AA}$ , and  $V = 2005.2(2) \text{ \AA}^3$  was selected. Data collection strategy was chosen for 100% completeness and redundancy of 3.9. Data reduction and analysis were carried out with the CrysAlisPro program [16]. Lorentz and polarization corrections were applied to intensity data using WinGX [17]. Reliable model with satisfactory R-values was obtained using the *P2/m* space group and it was chosen for the refinement. For the framework atoms, starting coordinates were taken from [18], and the extra-

**Table 1.** Experimental details for harmotome from Zlatolist

Parameter	Sample	Harmotome (this study) P121/m1
$a$ [ $\text{\AA}$ ]		9.8903(5)
$b$ [ $\text{\AA}$ ]		14.1394(3)
$c$ [ $\text{\AA}$ ]		8.6713(4)
$\beta$ [ $^{\circ}$ ]		124.628(7)
$V$ [ $\text{\AA}^3$ ]		997.81(8)
N $^{\circ}$ of reflections		8642
$R_{\text{int}}$		0.0266
$R_{\text{sigma}}$		0.0344
$h$ min		-12
$h$ max		13
$k$ min		-20
$k$ max		18
$l$ min		-9
$l$ max		13
theta min [ $^{\circ}$ ]		2.85
theta max [ $^{\circ}$ ]		32.82
unique reflections		3516
Ref. $F_o > 4\text{sig}F_o$		3099
N $^{\circ}$ of parameters		156
$R_1$		0.0403
$R_{\text{(all)}}$		0.0473
Goof		1.064

framework cations and water molecules were then assigned from the difference Fourier list. Structure refinements were performed using the program SHELXTL [17], employing neutral atomic scattering factors. Due to the Si, Al disorder, tetrahedral positions were later refined with Si scattering factors. Extraframework cations and water molecules were first refined using isotropic temperature factors. Each occupancy parameter was refined by fixing the occupancies of the remaining atoms. At the final stage of refinement, anisotropic temperature factors were introduced. Unit cell dimensions and experimental details are given in Table 1.

The analysis of measured intensity peaks and diffraction patterns confirmed that the sample is harmotome (Fig. 2, PDF Card 00-053-1175) [19]. Atomic coordinates, thermal displacement parameters, T–O–T angles, and T–O bond lengths, acquired from the X-ray single crystal measurement are listed in Tables 2-4.

The structure of harmotome from Zlatolist has a phillipsite-type framework with chains of four-membered rings, parallel to the  $a$ -axis (Fig. 3). The arrangement of Si, Al tetrahedra leads to the formation of three types of eight-membered rings, running along the three axes. Barium cations occupy the centre of the channels, parallel to the  $c$ -axis.

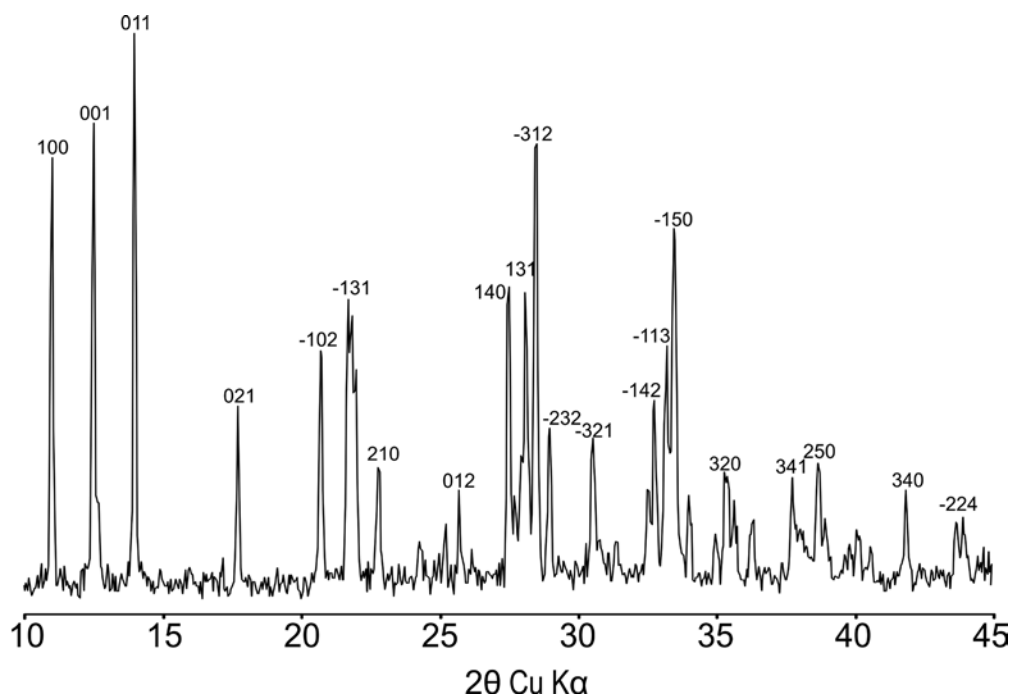


**Fig. 2.** Powder pattern of harmotome from Zlatolist. All intensity peaks correspond to the diffraction pattern of harmotome (PDF Card 00-053-1175)

Barium is coordinated by seven O atoms from the framework ( $2 \times O1$ ,  $2 \times O3$ ,  $2 \times O5$ , and  $O9$ ) and by four water molecules ( $W1$ ,  $W2$ , and  $2 \times W3$ ). Two of the five refined water molecules ( $W4$  and  $W5$ ) are disordered and are not bonded to barium, similar to [18].

#### MORPHOLOGICAL PROPERTIES

Harmotome from Zlatolist is transparent with vitreous luster, and though crystals are typically colourless, some fragments may be yellow-brownish or pale beige. Crystal size ranging from several mm to

**Table 2.** Atomic coordinates,  $U_{iso}$  ( $U_{eq}$ ) parameters and occupancies for harmotome

Label	x	y	z	$U_{iso}$ or $U_{eq}$	Occ.
T1	-0.05692(10)	-0.00826(6)	0.73246(10)	0.01031(16)	1
T2	0.12075(10)	0.13889(6)	0.58390(10)	0.0110(6)	1
T3	0.42053(10)	0.14073(6)	0.90646(10)	0.00990(16)	1
T4	0.26340(10)	-0.02459(6)	1.04746(11)	0.0105(6)	1
Ba	0.86210(5)	$\frac{1}{4}$	0.16707(4)	0.02476(11)	0.93
O1	0.6148(3)	0.11714(19)	0.9344(3)	0.0207(5)	1
O2	0.0960(3)	-0.05218(18)	0.8903(3)	0.0192(5)	1
O3	0.2190(3)	-0.0137(2)	1.2151(3)	0.0225(5)	1
O4	0.4111(5)	$\frac{1}{4}$	0.9672(5)	0.0230(7)	1
O5	0.3516(3)	0.07257(19)	1.0193(3)	0.0232(5)	1
O6	-0.0049(3)	0.0915(2)	0.6651(4)	0.0269(6)	1
O7	0.3119(3)	0.1291(2)	0.7102(3)	0.0234(5)	1
O8	0.0666(5)	$\frac{1}{4}$	0.5432(5)	0.0261(8)	1
O9	0.1035(4)	0.0921(2)	0.4077(4)	0.0318(6)	1
W1	0.8845(10)	$\frac{1}{4}$	0.8450(9)	0.0621(19)	1
W2	1.1986(10)	$\frac{1}{4}$	0.1881(10)	0.071(2)	1
W3	0.6983(7)	0.1375(4)	0.3277(6)	0.0702(14)	1
W4	0.532(3)	$\frac{1}{4}$	0.548(3)	0.124(12)	0.38
W5	0.508(2)	0.048(3)	0.4793(19)	0.21(2)	0.42

**Table 3.** Anisotropic displacement parameters for harmotome

Label	$U_{11}$	$U_{22}$	$U_{33}$	$U_{23}$	$U_{13}$	$U_{12}$
T1	0.0102(3)	0.0119(4)	0.0090(3)	-0.0007(3)	0.0035(3)	-0.0004(3)
T2	0.0137(7)	0.0087(7)	0.0096(7)	-0.0009(3)	0.0030(3)	-0.0013(3)
T3	0.0081(3)	0.0076(3)	0.0132(4)	0.0010(3)	0.0028(3)	0.0002(3)
T4	0.0087(7)	0.0115(7)	0.0119(7)	0.0016(3)	0.0044(4)	0.0008(3)
Ba	0.0331(2)	0.01613(16)	0.02686(19)	0.000	0.01274(14)	0.000
O1	0.0136(10)	0.0204(11)	0.0284(13)	0.0037(10)	0.0077(9)	0.0037(9)
O2	0.0157(10)	0.0199(11)	0.0189(11)	0.0009(9)	0.0022(9)	0.0015(9)
O3	0.0166(10)	0.0338(14)	0.0168(11)	-0.0005(10)	0.0055(9)	0.0034(10)
O4	0.0327(19)	0.0117(14)	0.0265(18)	0.000	0.0129(15)	0.000
O5	0.0241(12)	0.0191(11)	0.0290(13)	0.0032(10)	0.0126(10)	-0.0049(9)
O6	0.0253(12)	0.0248(13)	0.0350(15)	0.0115(11)	0.0161(11)	-0.0009(10)
O7	0.0185(11)	0.0310(13)	0.0168(11)	-0.0001(10)	0.0012(9)	0.0015(10)
O8	0.0246(18)	0.0143(15)	0.036(2)	0.000	0.0063(16)	0.000
O9	0.0386(16)	0.0336(15)	0.0237(13)	-0.0127(12)	0.0117(12)	-0.0067(13)
W1	0.103(5)	0.033(3)	0.078(5)	0.000	0.066(4)	0.000
W2	0.079(5)	0.078(5)	0.076(5)	0.000	0.053(4)	0.000
W3	0.070(3)	0.092(4)	0.056(3)	0.013(3)	0.031(2)	-0.006(3)
W4	0.104(18)	0.23(4)	0.086(16)	0.000	0.089(16)	0.000
W5	0.039(6)	0.33(7)	0.044(8)	-0.012(17)	0.016(6)	-0.058(17)

**Table 4.** T–O bond lengths [Å] and T–O–T angles [°] for tetrahedra of harmotome

T–O bond	Distance [Å]	T–O bond	Distance [Å]	T–O–T angle	Angle [°]
T1 – O9	1.646(3)	T3 – O5	1.631(3)	T3–O1–T4	139.36(18)
T1 – O6	1.650(3)	T3 – O5	1.642(3)	T4–O2–T1	144.14(17)
T1 – O3	1.652(3)	T3 – O4	1.6440(16)	T4–O3–T1	138.65(17)
T1 – O2	1.658(2)	T3 – O1	1.650(2)	T3–O4–T3	140.0(3)
mean	1.652(3)	mean	1.642(3)	T3–O5–T4	151.3(2)
T2 – O9	1.626(3)	T4 – O5	1.632(3)	T2–O6–T1	144.1(2)
T2 – O6	1.635(3)	T4 – O3	1.640(3)	T2–O7–T3	139.69(19)
T2 – O7	1.642(3)	T4 – O2	1.653(2)	T2–O8–T2	146.1(3)
T2 – O8	1.642(1)	T4 – O1	1.654(3)	T2–O9–T1	155.2(2)
mean	1.636(3)	mean	1.645(3)		

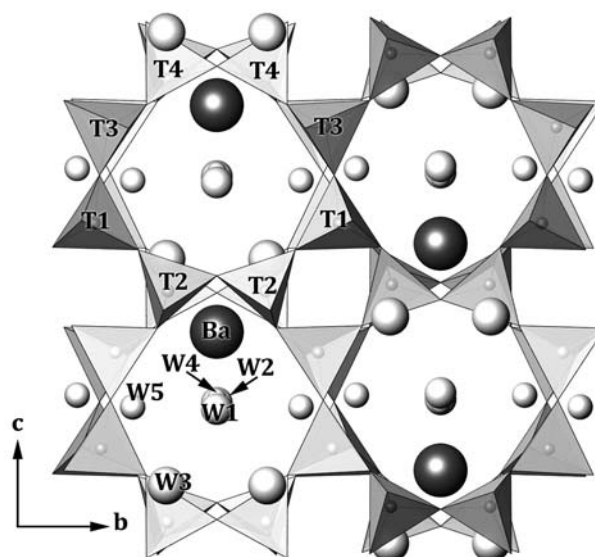


**Fig. 3.** The atomic structure of harmotome from Zlatolist, projected along the *a*-axis. Size of spheres corresponds to site occupancies, larger spheres have higher occupancies. T stands for tetrahedral site, W – water molecule

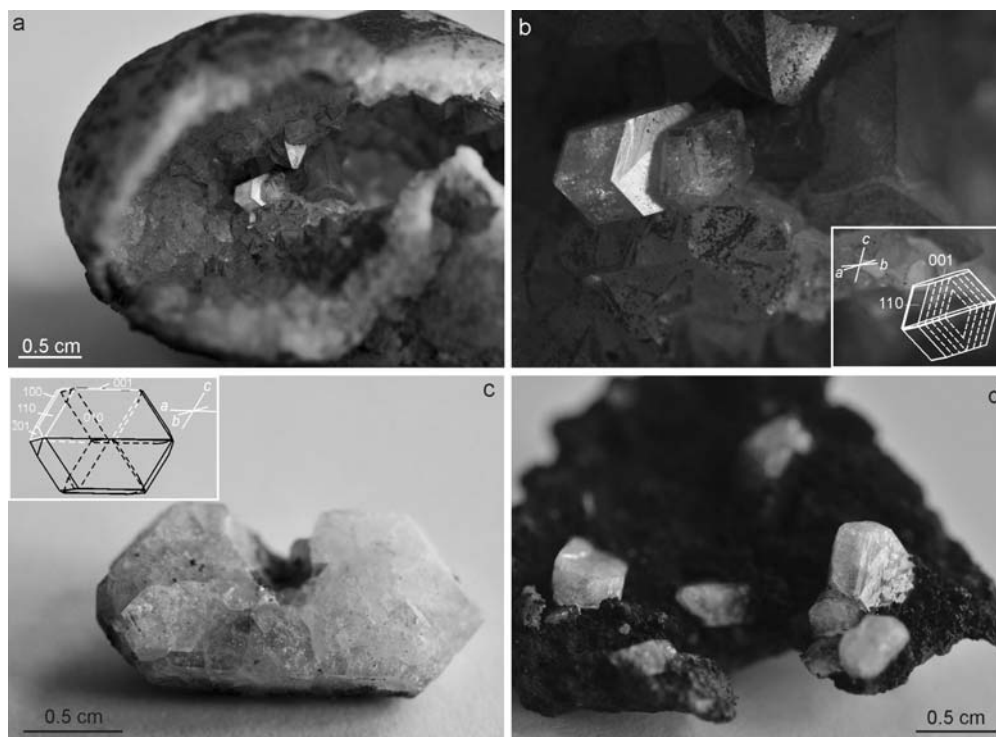


**Fig. 4.** Morphology of harmotome crystals: a) small amygdale partially filled by quartz, analcime and harmotome; b) twin variety after so-called morvenite law according to the characteristic striae parallel to the edge between  $\{010\}$  and  $\{110\}$  and twin suture running parallel to  $\{001\}$ ; c) pseudo-orthorhombic twin, composed by four individuals; d) transparent crystals with oriented, stepped hillocks on  $\{010\}$  faces

1.5 cm (Figs 4, 6). Large crystals up to  $\sim 3.5$  cm have been collected rarely.

Optical and SEM observations indicate that the mineral prevalently forms penetration twins without re-entrant angles. The crystal habit is characterized by short prismatic pseudo-orthorhombic forms. Equant crystals and radiating aggregates are common. The

crystals are always pseudo-orthorhombic penetration twins. Twinning suture and combination striations can be detected on each crystal (Fig. 4b-d). Judging from the values of interfacial angles, the presence of characteristic striae parallel to the edge between  $\{010\}$  and  $\{110\}$  and twin suture running parallel to  $\{001\}$  the twin variety form pseudo-orthorhombic

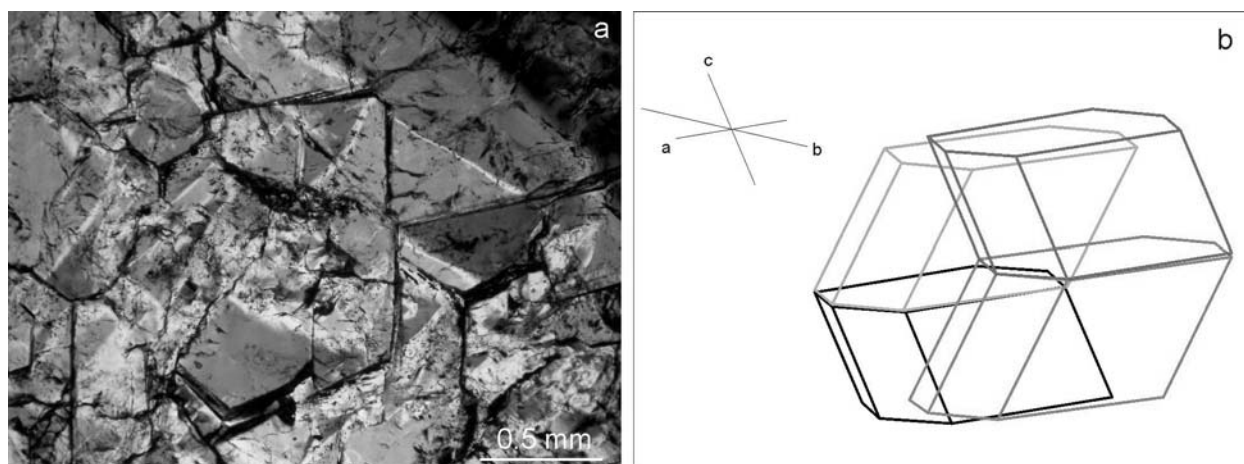


**Fig. 5.** Crystallographic characteristics: a) microphotograph with characteristic uneven extinction, thin section under crossed polars; b) habit of a simple penetration twin

penetration twins after the so-called morvenite law. Complex twinning results in an optical heterogeneity and shows characteristic uneven extinction under crossed polars (Fig. 5a).

The morvenite twin is a fourling twin, present in all investigated crystals and without re-entrant angles. It is composed of four individuals (Fig. 5b), ar-

ranged across the twin planes (001) and (20 $\bar{1}$ ), displaying the {100}, {010}, {001}, {110}, and small {201} forms. The four sets of intersecting striations, which indicate the presence of the four individuals, are seen only on the (010) faces. Morvenite twins are commonly elongated along the  $a$ -axis, and flattened on the {010}.

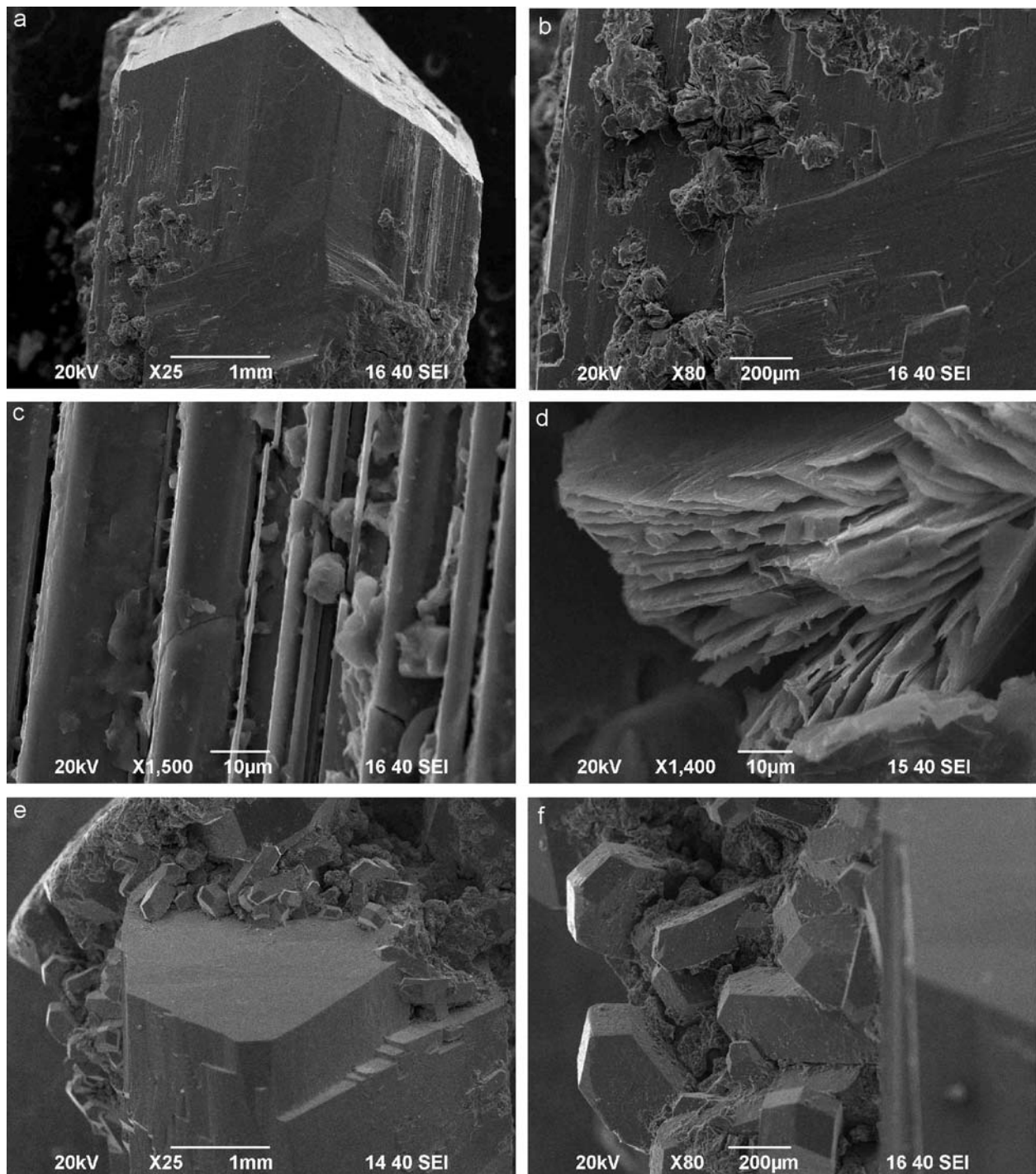


Fig. 6. SEM images of: a-c) harmotome crystal surface; d) a detail showing partial replacement by chlorite; e-f) groups of small twinned individuals on large pseudo-orthorhombic crystal from one amygdale

Under SEM it is revealed that mineral surfaces of some crystals are decorated by spherulitic aggregates (Fig. 6b–d), probably after partial replacement by chlorite (?).

### CHEMICAL COMPOSITION

The average chemical formula based on EPMA is as follows:  $Ba_{2.46}Ca_{0.17}K_{0.26}[Al_{5.89}Si_{10.19}O_{32}] \cdot 12H_2O$ . Calcium and potassium are both conspicuous in the chemical composition of the harmotome studied (Table 5). Sodium, magnesium and iron often reported in harmotome [20, 21] was not found using EPMA. Additionally, the mineral analysed is characterized by distinctly higher amounts of aluminium and barium than those cited in the literature. Si/(Si+Al) ratio shows an average value of 0.71 in Zlatolist, and ranges from 0.68 in crystals from trachyandesite of Iskra, Bulgaria [14], to 0.76 in crystals from basalts of Weitendorf, Austria [22]. According to the average ratio (Ra) after Passaglia and Sheppard [23]

and experimentally determined in this study Ra=0.63 harmotome can be classified as intermediate zeolite.

Data are “reliable”, i.e. with the content of tetrahedral cations (Si+Al) close to half of the oxygen atoms and the balance error  $E = [(Al - Al_{theor.}) / Al_{theor.}] \times 100$  lower than 10% [24].

Chemical analyses were performed by electron microprobe and the water content is the result of normalization of data to 100%. The number of water molecules is known to be related to both structural and chemical parameters because it increases with Si/Al and divalent/monovalent cation ratios. Contents of H<sub>2</sub>O tend to decrease with increasing number and size of extra-framework cations, as well as with increasing temperature and decreasing P(H<sub>2</sub>O). Such variations can be vital to petrological, geochemical, environmental, and experimental considerations [6].

Minor and trace elements in harmotome are registered also by LA-ICP-MS. Determined are up to 1.3 wt.% Na, 1.2 wt.% K, and 0.6 wt.% Ca. Traces of: Sr (330), V (100), Rb (65), Ti (26), Zn (20), Mn (16), Cu (15), P (15), Fe (14) in ppm are found.

**Table 5.** Chemical analyses and formulae on the basis of 32 oxygens

wt.%	Bar1 p.1	Bar1 p.2	Bar1 p.3	Bar2 p.1	Bar2 p.2	Bar2 p.3	Bar3 p.1	Bar3 p.2
Al <sub>2</sub> O <sub>3</sub>	18.42	18.68	22.18	18.29	18.11	21.72	18.57	18.65
SiO <sub>2</sub>	39.53	40.55	38.3	39.04	40.81	37.99	39.91	39.23
K <sub>2</sub> O	0.34	0.51	0.6	0.95	0.82	1.58	0.85	0.58
CaO	0.63	1.68	0.25	0.42	0.46	0.71	0.15	0.56
BaO	25.68	23.42	23.41	25.87	25.64	21.72	25.28	25.37
MnO	–	0.19	0.16	–	0.15	0.25	0.08	0.15
Total	84.6	85.03	84.9	84.57	85.99	83.97	84.84	84.54
H <sub>2</sub> O*	15.4	14.97	15.1	15.43	14.01	16.03	15.16	15.46
*–H <sub>2</sub> O by difference to approx. 100 wt.% total								
Weight % – analyses computed to 100% without H <sub>2</sub> O								
Al <sub>2</sub> O <sub>3</sub>	21.77	21.97	26.12	21.63	21.06	25.87	21.89	22.06
SiO <sub>2</sub>	46.73	47.69	45.11	46.16	47.46	45.24	47.04	46.40
K <sub>2</sub> O	0.40	0.60	0.71	1.12	0.95	1.88	1.00	0.69
CaO	0.74	1.98	0.29	0.50	0.53	0.85	0.18	0.66
BaO	30.35	27.54	27.57	30.59	29.82	25.87	29.80	30.01
MnO	0.00	0.22	0.19	0.00	0.17	0.30	0.09	0.18
Total	100.00	100.00	100.00	100.00	100.00	100.00	100.00	100.00
Number of cations on the bases of 32 oxygen equivalents, ignoring H <sub>2</sub> O								
Al	5.67	5.65	6.65	5.67	5.47	6.56	5.68	5.74
Si	10.32	10.42	9.75	10.27	10.46	9.73	10.36	10.25
K	0.11	0.17	0.20	0.32	0.27	0.52	0.28	0.19
Ca	0.18	0.46	0.07	0.12	0.13	0.20	0.04	0.16
Ba	2.63	2.10	2.33	2.67	2.58	2.18	2.57	2.60
Mn	0.00	0.04	0.03	0.00	0.03	0.05	0.02	0.03
Si/(Si+Al)	0.65	0.65	0.59	0.64	0.66	0.60	0.65	0.64
K/(K+Ba)	0.04	0.07	0.08	0.11	0.09	0.19	0.10	0.07
E%	–5.56	–5.76	10.84	–5.45	–8.81	9.34	–5.35	–4.28

The thermal behavior of harmotome, from TG-DTA-DTG measurements, with five different water sites in the structure, represents water loss in three steps: at 125, 210, and 280 °C, and complete dehydration at 400 °C.

#### GENETIC AND CONCLUDING REMARKS

Zeolites can originate from a variety of precursor materials including volcanic and impact glasses, aluminosilicate minerals including other zeolites, smectite, feldspars and feldspathoids [25]. Most of the famous zeolite specimens known from the mineral collections are incrustations on the walls of geodes and vugs of basic lavas (basalts sensu lato). The genesis of these crystals could be considered, as those occurring in non-volcanic rocks, due to hydrothermal deposition [26]. Harmotome is known to have both sedimentary and hydrothermal origin; the second one being by far the most common [1, 25, 27]. However, zeolitic rocks, widespread in Eastern Rhodopes, are known as product of volcanic glass and pyroclastics transformation. Zeolites form more rapidly from glass than from crystalline materials, and the reaction rate of glass varies inversely with its silica content [28]. Most of the features of Zlatolist zeolites differ compared to microcrystalline zeolites formed in sediments. Well-developed large crystals, number of zeolite species and average chemical composition are indicative for hydrothermal origin, according to the criteria suggested by Gottardi [26].

The source of barium, the element necessary in the formation of harmotome, could be barite concretions in adjacent pyroclastic rocks. Also, in some basic to intermediate rock varieties from the volcanic complex Ba-content up to 1970 ppm was determined [29]. Barium could have been derived from feldspars, common in the volcanic varieties of the area, as well. Moreover, Ba-sanidine with up to 8.9 wt.% BaO was recently described by Yanev and Ivanova [30] from the acid volcanic varieties from the adjacent region in the Eastern Rhodopes.

Finally, the co-existence of the Zlatolist harmotome with chalcedony, quartz and calcite crystals and its occurrence in geodes indicates the hydrothermal, probably low temperature, origin of the mineral with a transport of the substance at some distance.

**Acknowledgements:** The authors would like to express thanks to Stela Atanassova (Institute of Physical Chemistry, BAS) for SEM/EDS analyses and Vilma Petkova (Institute of Mineralogy and Crystallography, BAS) for DTA measurements.

#### REFERENCES

1. G. Gotardi, E. Galli, in: Natural zeolites, Springer-Verlag, 1985, p. 135.
2. A. Corma, *Chem. Rev.*, **95**, 559 (1995).
3. Z. A. D. Lethbridge, J. J. Williams, R. I. Walton, K. E. Evans, C. W. Smith, *Micropor. Mesopor. Mater.*, **79**, 339 (2005).
4. R. Brent, M.W. Anderson, *Angew. Chem. Int. Ed.*, **47**, 5327 (2008).
5. M. H. F. Kox, E. Stavitski, B. M. Weckhuysen, *Angew. Chem. Int. Ed.*, **46**, 3652 (2007).
6. D. Coombs, A. Alberti, T. Armbruster, G. Artioli, C. Colella, E. Galli, J. D. Grice, F. Liebau, J. A. Mandarino, H. Minato, E. H. Nickel, E. Passaglia, D. R. Peacor, S. Quartieri, R. Rinaldi, M. Ross, R. A. Sheppard, E. Tillmanns, G. Vezzalini, *Canadian Mineralogist*, **35**, 1571 (1997).
7. W. A. Deer, R. A. Howie, J. Zussman, Rock-forming minerals, vol. 4, Framework silicates, Longman, London, 1963.
8. Th. G. Sahama, M. Lehtinen, *Mineralogical Magazine*, **36**, 444 (1967).
9. M. Akizuki, *American Mineralogist*, **66**, 403 (1981).
10. M. Akizuki, *American Mineralogist*, **70**, 822 (1985).
11. T. Thomson, Outlines of Mineralogy, geology and mineral analysis, vols. I and II, London, 1836.
12. R. Tschernich, Zeolites of the World, Geoscience Pres., Arizona, 1992.
13. T. Armbruster, M. Gunter, in: Natural Zeolites: Occurrence, Properties, Applications, D. L. Bish, D. W. Ming (eds.), vol 45, Mineralogical Society of America, Virginia, 2001, p. 217.
14. I. Kostov, *Annu. Univ. Sofia, Fac. Biol. Geol. Geogr.* livre 2, Geol., **55**, 159 (1962).
15. Y. Yanev, J.-J. Cochemé, R. Ivanova, O. Grauby, E. Burel, R. Pravchanska, *N. Jb. Miner. Abh.*, **182**(3), 265 (2006).
16. Oxford Diffraction. CrysAlis PRO, Oxford Diffraction Ltd, Yarnton, England, 2010.
17. G. M. Sheldrick, *Acta Crystallographica A*, **64**, 112 (2008).
18. E. Stuckenschmidt, H. Fuess, A. Kvik, *European Journal of Mineralogy*, **2**, 861 (1990).
19. J. Faber, T. Fawcett, *Acta Crystallographica B*, **58**, 325 (2002).
20. R. Rinaldi, J. J. Pluth, J. V. Smith, *Acta Crystallographica B*, 2426 (1974).
21. P. Cherny, R. Rinaldi, R.C. Surdam, *Neues Jahrb. Miner. Abh.*, **128**(3), 312 (1977).
22. T. Armbruster, M. Wenger, T. Kohler, *Mitt. Abt. Mineral. Landesmus.*, **59**, 13 (1991).
23. E. Passaglia, R. A. Sheppard, in: Natural Zeolites: Occurrence, Properties, Applications, D. L. Bish, D. W. Ming (eds.), vol 45, Mineralogical Society of America, Virginia, 2001, p. 69.
24. E. Passaglia, *American Mineralogist*, **55**, 1278 (1970).
25. R. L. Hay, R. A. Sheppard, in: Natural Zeolites: Occurrence, Properties, Applications, D. L. Bish, D. W. Ming (eds.), vol 45, Mineralogical Society of America, Virginia, 2001, p. 217.

26. G. Gottardi, *European Journal of Mineralogy*, **4**, 479 (1989).
27. T. Wieser, *Mineralogia Polonica*, **16**, 3 (1985).
28. R. A. Sheppard, R. L. Hay, in: Natural Zeolites: Occurrence, Properties, Applications, D.L. Bish, D.W. Ming (eds.), vol 45, Mineralogical Society of America, Virginia, 2001, p. 261.
29. Y. Yanev, R. Ivanova, *Geochemistry, Mineralogy and Petrology*, **48**, 39 (2010).
30. B. Yardonov, S. Sarov, S. Georgiev, V. Valkov, E. Balkanska, V. Grozdev, R. Marinova, N. Markov, *Explanatory note to the Geological Map of the Republic of Bulgaria Scale 1:50 000*, 2008, p. 124.

## КРИСТАЛОГРАФСКИ, ХИМИЧНИ И СТРУКТУРНИ ХАРАКТЕРИСТИКИ НА ХАРМОТОМ ОТ ЗЛАТОЛИСТ, ИЗТОЧНИ РОДОПИ, БЪЛГАРИЯ

Р. Атанасова<sup>1\*</sup>, Р. Д. Василева<sup>1</sup>, М. Кадийски<sup>2</sup>, З. Златев<sup>3</sup>

<sup>1</sup>Геологически институт, Българска академия на науките, 1113 София;

<sup>2</sup>Институт по минералогия и кристалография, Българска академия на науките, 1113 София;

<sup>3</sup>Българско минералогическо дружество, София

Постъпила на 15 февруари, 2012 г.; приета на 15 март, 2012 г.

(Резюме)

През палеогена големи количества от средни и кисели вулканокластични скали са отложени в Източните Родопи, Южна България. Повечето от тях са образувани в плиткоморски условия и в следствие са трансформирани в глини, адулар, опал-СТ и zeoliti. Интересна минерализация беше установена в празнини и кухини на базалтови андезити в района на с. Златолист. Празнините, сега миндали са запълнени с калцит, кварц и разнообразни zeoliti (хармотом, аналцим, морденит, хейландит и др.). Сред тях хармотомът се отличава със забележителни добре оформени кристали с размер достигащ до 3,5 cm.

Хармотомът е характеризирани с оптична микроскопия, прахова и монокристална рентгенография, SEM/EDS, микросондови анализи, LA-ICP-MS и DTA. Изследваните кристали неизменно са изградени от комплексни проникващи двойници. Двойникуването симулира псевдоромбични форми съгласно морвени-тов закон на срастване. Кристалите са удължени по *a*-оста и с плочесто развитие по {010}. Това комплексно двойникуване се отразява на оптичната хетерогенност и анизотропия.

Средната кристалохимична формула е:  $\text{Ba}_{2.46}\text{Ca}_{0.17}\text{K}_{0.26}[\text{Al}_{5.89}\text{Si}_{10.19}\text{O}_{32}]\cdot 12\text{H}_2\text{O}$ . Определени са и 35 елементи-примеси и следи: до 1.3 тегл.% Na, 330 ppm Sr, and 26 ppm Ti. Термичното поведение на хармотома се изразява в загуба на вода на три стъпки: при 125, 210, и 280 °C. Окончателна дехидратация се достига при 400 °C.

Кристален фрагмент от хармотом е характеризирани с монокристална рентгенова дифрактометрия. Добър модел с удовлетворителни стойности на R ( $R1 = 0.0403$ ;  $R(\text{all}) = 0.0473$ ) е достигнат с използване на пространствената група P2/m, която е избрана за структурни уточнения. Получените параметри на елементарна клетка са:  $a = 9.8903(5)$ ,  $b = 14.1394(3)$ ,  $c = 8.6713(4)$  Å,  $\beta = 124.628(7)^\circ$  и  $V = 997.81(8)$  Å<sup>3</sup>. Финалните уточнения включват всички атомни координати и анизотропни термични параметри.